2D separations on a 1D chip: gradient elution moving boundary electrophoresis—chiral capillary zone electrophoresis†

David Ross,* Jonathan G. Shackman,‡ Jason G. Kralj and Javier Atencia

Received 31st March 2010, Accepted 24th August 2010
DOI: 10.1039/c004819d

A new method is described for two-dimensional (2D) separations using a microfluidic chip normally employed for single dimension electrophoresis. The method employs a combination of gradient elution moving boundary electrophoresis (GEMBE) and chiral capillary zone electrophoresis (CZE). The simplicity of the first dimension GEMBE method enables its implementation in the injection channel of a conventional electrophoresis chip, simplifying the design and operation of the device. The method was used for high resolution 2D chiral separations of a mixture of amino acids considered as possible signatures of extant or extinct life for solar system exploration. The enantiomers of aspartic acid, glutamic acid, serine, alanine, and valine were all resolved as well as glycine (achiral) and several unidentified impurities, giving an estimated peak capacity of 35 for the region between valine and glycine. The results highlight the need for high peak capacity separations for chiral amino acid analysis if accurate enantiomeric ratios are to be determined.

Introduction

One of the primary figures of merit for analytical separations of complex samples is the peak capacity, or the maximum number of analytes that can be resolved if the analyte peaks are uniformly distributed. For real analyses, with non-uniform peak spacing, Giddings has shown that the number of components (s) that can typically be resolved by a separation is given by:

$$s = m \times \exp\left(-\frac{2m}{n_c}\right) \quad (1)$$

where n_c is the peak capacity and m is the total number of components in the mixture.[1] For separations requiring high peak capacities, multidimensional separation techniques are often used, since they can provide a greater improvement in peak capacity per unit time than simply using a longer separation column with a 1D separation. If the selectivities of the different separations used for a multidimensional technique are uncorrelated, the separations are said to be orthogonal, and the total peak capacity is given by the product of the peak capacities of the individual separations.[1,2]

The prototypical multidimensional separation technique is 2D polyacrylamide gel electrophoresis (2D-PAGE),[3] which has been a workhorse technique for proteomics studies for over 30 years. With 2D-PAGE, peak capacities of 5000 or even higher are possible. However, the technique is laborious, slow, and has a limited dynamic range. Consequently, a number of research groups have worked to develop alternative 2D separation methods.

National Institute of Standards and Technology, 100 Bureau Dr, Gaithersburg, MD, 20899, USA. E-mail: david.ross@nist.gov; Tel: +1-301-975-2525

† Electronic supplementary information (ESI) available: Additional data and raw data. See DOI: 10.1039/c004819d

‡ Current address: Department of Chemistry, Temple University, 1901 N. 13th St, Philadelphia, PA, 19122, USA.

With 2D-PAGE the orthogonal separations are performed sequentially. The analyte fractions are transferred to the second dimension only after completion of the first dimension separation; and all of the second dimension separations are run at the same time, in parallel. An alternative approach to 2D separations is for fractions to be transferred from the first dimension to the second in a serial fashion, one at a time. This approach is typically used for multidimensional capillary electrophoresis or column chromatography such as GC-GC, LC-LC, LC-CE, or CE-CE.[4–12] With both parallel and serial approaches to multidimensional separations, the interface between the separation dimensions is an important consideration. The fractions must be transferred from the first dimension separation to the second dimension separation (and additional dimensions, if applicable) with minimal added dispersion. Because of the advantages offered by microfluidic technologies for integrating multiple analysis steps (including multiple separations) with minimal dead volume or added dispersion, much of the recent work on novel 2D separation methods has taken place in the field of microfluidics.[13,14]

Although the performance of many of the 2D microfluidic methods has been impressive, they typically require complex microchannel geometries and operational procedures. For example, serial integration of micellar electrokinetic chromatography (MEKC) and capillary zone electrophoresis (CZE) on a microchip, first demonstrated by Rocklin *et al.*[15] and Ramsey *et al.*,[16] was shown to provide very high peak capacity (500 to 4200, generated in 10 min to 15 min), and the reproducibility was suitable for proteomics applications. However, it required a device with long microfluidic channels, and independent control of at least six high voltage sources. Other techniques have been described that require microfluidic devices with a large number of injection crosses[17–23] and/or various manual manipulations, such as solution switching or device disassembly at various points during the separation.[17–21,24–29] For a more complete overview of multidimensional separations in

microfluidic systems, see the recent reviews by Tia and Herr,[13] and Chen and Fan.[14]

Although most work on microfluidic 2D separations has focused on proteomics separations, there have been a few recent reports of 2D methods directed at amino acid separations. For example, Xu *et al.*[30] used a device similar to that described by Rocklin *et al.*[15] and Ramsey *et al.*[16] for 2D MEKC-CZE separation of amino acids with a reported peak capacity of approximately 115 (generated in 20 min); Kim *et al.*[31] described a method for 2D CZE-chiral CZE implemented with a track-etched polycarbonate membrane to control the transfer of analytes from the CZE channel to the chiral CZE channel.

In the last ten years, several publications, primarily from the Mathies group, have described efforts to develop a microfluidic chip-based platform for analysis of extraterrestrial samples in the search for signs of life on Mars and elsewhere in the solar system.[32–42] One of the primary objectives for that work is to develop the capability to accurately measure the enantiomeric ratio of amino acids found in extraterrestrial samples. Most amino acids exist in two forms, or enantiomers, which are non-superimposable mirror images of each other. In abiotic conditions amino acids synthesis typically leads to a racemic mixture, with equal concentrations of each enantiomer. However, in biological systems (life), amino acids are predominantly presented in one form (the L-enantiomer for terrestrial life).[43] Consequently, the detection of amino acids with a predominance of one enantiomer over the other could give clues of extant or extinct life, and amino acids are therefore considered as important biomarkers in the search for signs of extraterrestrial life.[44] Accurate measurement of enantiomeric excess, however, requires a separation mode capable of resolving all or most of the different amino acid enantiomers that would be found in a sample. Using only those amino acids that are commonly found either in meteorites[45] or in living systems on Earth as an estimate of the number of possible analytes present, the chiral separation would need to resolve about 50 components. From eqn (1), it is clear then that a high peak capacity technique would be required (>150 to resolve just one half of the components).

The goal of this work was to explore the possibility of implementing a fully automated 2D separation using a simplified microfluidic system with minimal voltage control points and injection crosses for high peak capacity chiral separations. The 2D separation was applied to the problem of chiral amino acid analysis and evaluated for its peak capacity and ability to resolve a mixture of amino acid enantiomers. The simplified method that was developed used a combination of gradient elution moving boundary electrophoresis (GEMBE)[46] and chiral CZE for chiral amino acid separations with an estimated peak capacity of 35 for the region between valine and glycine.

GEMBE is a recently described method for electrophoretic separations in a microfluidic system that is simple to implement and robust in operation. GEMBE requires only a simple, short microfluidic channel or capillary connecting two reservoirs (sample and background buffer). Separations are achieved by balancing the electrophoretic motion of analytes against a bulk solution counterflow that is varied over time. Initially, the counterflow is set so that the analytes of interest all remain in the sample reservoir and do not enter the separation channel. As the counterflow velocity is varied, each analyte, in turn, is allowed to enter the channel where it is detected as a moving boundary or step change in the detector signal. In contrast with conventional electrophoretic methods, all of the analytes take the same amount of time to travel from the channel entrance to the detection point, but they are resolved because they enter the microchannel at different times. Thus the selectivity of the method occurs primarily at the channel entrance, and the resolution is only weakly dependent on the channel length. Consequently, short microchannels can be used,[47,48] significantly reducing the required footprint of the microfluidic device. In addition, because the counterflow can be used to exclude many matrix interferents such as proteins or particulates from entering the separation channel, the GEMBE method can be used to analyze difficult samples with minimal sample preparation.[49]

Because of the simplicity of the GEMBE method, a 2D GEMBE-CZE separation can be implemented using a microfluidic device normally used for conventional, 1D microchip CZE. For the method described here, the required instrumentation is further simplified by using a CZE microchip layout designed to minimize the number of fluid reservoirs and voltage sources.[50] The device schematic is shown in Fig. 1. Because the GEMBE separation does not require a defined injection plug, there are only three fluid access reservoirs and a single injection cross. The GEMBE separation takes place in what would normally be the sample input arm of the chip, and analytes are transferred from the GEMBE channel to the CZE channel at the injection cross.

Experimental§

Chemicals and reagents

Carboxyfluorescein succinimidyl ester (5-FAM, SE) was purchased from Invitrogen (Carlsbad, CA). (2-Hydroxypropyl)-β-cyclodextrin (HP-β-CD), 0.6 molar substitution, molecular weight approximately 1380, Sigma Aldrich catalog number 332593 and all other chemicals were obtained from Sigma Aldrich (St Louis, MO). All solutions were made with water (resistivity > 18 MΩ cm) from a Barnstead (Dubuque, IA) Easypure II ultrapure water system.

The amino acid/primary amine mixtures used consisted of fluorescently labeled aspartic acid (asp), glutamic acid (glu), glycine (gly), alanine (ala), serine (ser), valine (val), methylamine, and propylamine. All were present in both D and L forms except the achiral gly, methylamine and propylamine. Stock solutions of the amine mixtures were prepared at 100 μmol L^{-1}, 10 μmol L^{-1} and 1 μmol L^{-1} concentrations of each of the amines and amino acids. Stock solution of 5-FAM, SE was prepared at a concentration of 0.1 mol L^{-1} in dimethyl sulfoxide. For labeling, 10 μL of dye stock were added to 990 μL of amino acid stock and incubated at room temperature for 12 hours in the dark. Following incubation, labeled amino acid solutions were stored

§ Certain commercial equipments, instruments, or materials are identified in this article to specify adequately the experimental procedure. Such identification does not imply recommendation or endorsement by the National Institute of Standards and Technology nor does it imply that the materials or equipment identified are necessarily the best available for the purpose.

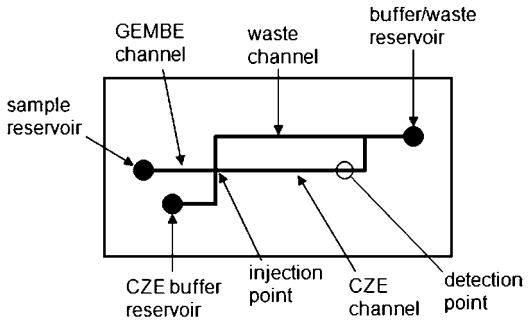

Fig. 1 Schematic for 2D separation chip. Sample is loaded into the sample reservoir, and CZE buffer (containing the chiral selector HP-β-cyclodextrin) is loaded into the CZE buffer reservoir. Pressure control is applied to the headspace of the buffer/waste reservoir. Negative high voltage is applied to the buffer/waste reservoir; the sample reservoir is grounded; and the CZE buffer reservoir is connected *via* a computer-controlled high voltage relay to either ground or to a smaller, positive high voltage.

at 5 °C until used. These solutions were used without removal of free dye as stock for separation experiments. In addition to the mixtures, each amine and amino acid was labeled separately to allow for peak identification. Labeled buffer blank samples were also prepared and analyzed for identification of dye hydrolysis products and other impurities. After labeling, mixtures were diluted into 0.25 mol L^{-1} tris-borate buffer, pH 8.3, for use. Dilution factors used were 50× (for Fig. 3) and 10× (for Fig. 4–7). The sample concentrations given below assume 100% yield for the labeling reaction. However, the degree of labeling was not characterized. Note that the 5-FAM, SE label is achiral, so that there is typically only one chiral center in each labeled amino acid molecule. Consequently, there are only two peaks in a chiral separation for each chiral amino acid.

Device fabrication

The microfluidic devices were fabricated from Borofloat glass using a previously described method.[51] Briefly, 1 mm thick photomask blanks (Telic Company, Valencia, CA) were used and etched in 14 : 20 : 66 (v/v/v) HNO_3/HF/H_2O to produce channels 30 μm wide and 7 μm deep. Access holes, 2.2 mm in diameter, were drilled with a diamond-tipped drill bit (LK Technologies, Inc., Cleveland, OH) using a bench-top computer numerical control (CNC) mill (Taig model 2019, Carter Tools, Philomath, OR). The etched substrate and matching cover plate were cleaned, assembled, and placed in a furnace at 610 °C for 8 h under a 400 g stainless steel weight for bonding.

Instrumentation

A reservoir with approximately 1.5 mL volume was clamped over the buffer/waste reservoir and sealed to the microfluidic chip with a polydimethylsiloxane (PDMS) gasket. The headspace pressure of the buffer/waste reservoir was controlled using a model APC-600 pressure controller (Mensor, San Marcos, TX). High voltage (−4000 V, Stanford Research System, Model PS350, Sunnyvale, CA) was also applied to the buffer/waste reservoir with a platinum electrode sealed into the reservoir. Smaller reservoirs (100 μL) were attached to the sample reservoir and the CZE buffer reservoir, also with PDMS gaskets. To slow evaporation during operation, both the CZE buffer reservoir and the sample reservoir were covered with small PDMS sheets which were cut in an 'X' pattern to allow insertion of the platinum electrodes for electrical connections. The sample reservoir was electrically grounded with a platinum electrode. The CZE buffer reservoir was connected to a second high voltage power supply set at +800 V *via* a computer-controlled relay that was used to control the injections into the CZE channel.

The microfluidic device and reservoirs were mounted on a plate held above an inverted laser-induced fluorescence (LIF) detector similar to a previously described design.[52] A solid state 488 nm laser (model CLAS-488-025-PP00, Blue Sky Research, Milpitas, CA) was used for excitation. The laser was directed through a 475 ± 40 nm bandpass filter and reflected by a 505 nm long-pass dichroic mirror through a 20×, 0.4 NA, long working distance, microscope objective (Carl Zeiss, Thronwood, NY) onto the detection point, 25 mm after the injection cross. Emission light was collected with the same objective and passed through the dichroic mirror and a 535 ± 45 nm bandpass filter toward a tube lens (plano-convex, $f = 100$ mm, Newport, Irvine, CA). Fluorescence emission was detected with a photomultiplier tube (PMT, R1477, Hamamatsu, Bridgewater, NJ) powered by a high voltage power supply (Stanford Research System, Model PS350, Sunnyvale, CA). PMT current was amplified and filtered (3 Hz low-pass) by a low-noise current preamplifier (Stanford Research System, Model SR570, Sunnyvale, CA) and sampled at 100 Hz using a 16-bit A/D board (USB-6229, National Instruments, Austin, TX). Instrument control and data acquisition were performed using a LabVIEW program written in-house (National Instruments).

Device operation

During sample and CZE buffer loading, the pressure applied to the buffer/waste reservoir was held at +60 kPa. After loading, both high voltage sources were turned on, the injection control relay was closed, and the pressure was reduced to +30 kPa for 6 seconds. The pressure was then reduced to the start pressure for each run and then ramped down at the specified rate until the end of a separation run. At the end of the run, the pressure was again increased to +60 kPa, and the high voltage sources were turned off. During the pressure ramp, the relay was periodically opened to inject analytes from the GEMBE channel to the CZE channel (see Fig. 2). The duration of each injection was 1 s, and the time between injections was set to avoid overlap of peaks from different injections.

Data analysis. Data were analyzed using software written in-house with Mathematica (Wolfram Research, Champaign, IL). Briefly, the data were first broken into individual electropherograms corresponding to each injection. The raw data (shown in the ESI†) were processed to find the positions in each electropherogram of 4 peaks that spanned the range of the electropherograms. Because the applied pressure was varied over time, the peak positions were not constant for each injection, but formed curved paths in the 2D plots of the raw data (Fig. S1–S4, ESI†). The positions of those 4 peaks were then used to convert

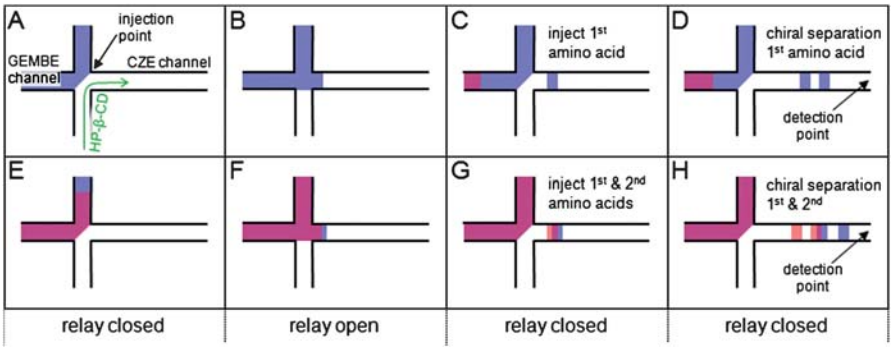

Fig. 2 Schematic of injection sequence at the interface between achiral GEMBE separation and chiral CZE separation. The figures show the region of the chip around the injection point (see Fig. 1). Amino acids are initially separated in the GEMBE channel and enter the injection region from the left in the figures. CZE buffer containing the chiral selector, HP-β-CD, flows into the injection region from the bottom channel. During most of the analysis, the relay is closed and the amino acids eluting from the GEMBE channel do not enter the CZE channel (A and E). During an injection, the relay is briefly opened to inject a plug of amino acids from the GEMBE channel into the CZE channel (B and F). After the relay is closed, the amino acids are separated based on chirality as they flow down the CZE channel (C and D and G and H). The figures show a sequence as two amino acids (shown as blue and red shading) sequentially elute from the GEMBE channel and are injected into the CZE channel. For the first injection (A–D) only the first amino acid is injected. For the second injection (E–H), both amino acids are injected. Even though two of the enantiomer peaks co-migrate in the CZE channel (the overlapping red and blue bands in H), all four enantiomer peaks can be individually detected by taking the difference between successive injections.

the x-axis from time to electrokinetic velocity using the following procedure. First, the migration times were fit to an equation derived to predict the shape of the curves assuming a constant acceleration (constant rate of change of applied pressure):

$$(t_{j,i} - t_{0,i}) = \frac{\sqrt{2L \times a + (a \times (t_{0,i} + B_i) + u_j)^2 - a \times t_{0,i} - u_j}}{a} \quad (2)$$

where $t_{j,i}$ was the elution time for peak j after injection i; $t_{0,i}$ was the time for each injection; and L was the distance between the injection cross and the detection point (25 mm). The adjustable parameters were: the bulk fluid acceleration (due to the linear pressure sweep rate), a; the velocity of each peak at time zero, U_j; and a parameter to allow for the slight timing variability of each injection, B_i. The best fit parameters were chosen to minimize the sum of the squared residuals for all 4 peaks simultaneously, using the same set of variability parameters (B_i) and acceleration (a) for the fits to all 4 lines. The resulting fit parameters were then used to rescale the x-axis of the electropherograms from time to CZE mobility (proportional to the U_j parameters plus a constant) for the 2D plots. The derivative plots (Fig. 3B, 4B, 5B, and 7B) were produced by taking the derivative of the rescaled 2D data along the vertical axis.

Results

The 2D method described here is based upon the use of GEMBE[46] with a device and method described by Jacobson *et al.*[50] for the minimization of the complexity of 1D microchip electrophoresis. A schematic of the chip design is shown in Fig. 1. The buffer/waste reservoir and channels were filled with run buffer (250 mmol L^{-1} tris-borate, pH 8.3). The CZE buffer reservoir was filled with the same buffer containing the chiral selector HP-β-CD at concentrations indicated in the figure captions. CZE and GEMBE with the same run buffer would normally have the same selectivity, so that no additional peak capacity would be gained by combining them in a 2D separation. However, the use of the chiral selector in the CZE buffer gives a different selectivity (based upon differing degrees of interaction between the analytes and the chiral selector) so that the combination of the achiral GEMBE separation with the chiral CZE separation gives a higher peak capacity than with either method used alone.

The 2D separation process is summarized schematically in Fig. 2. After sample loading, the high voltage and pressure control are turned on and a computer-controlled relay is periodically switched to inject sample from the GEMBE channel into the CZE channel. During operation a negative high voltage is applied to the buffer/waste reservoir and the sample is grounded. The CZE buffer reservoir is connected to a smaller, positive high voltage *via* a controlled high voltage relay. When the relay is closed, current and CZE buffer (driven primarily by electroosmosis) flow from the CZE buffer reservoir to the injection point and into the CZE channel (see Fig. 2A), and sample flows from the sample reservoir to the injection point and then into the waste channel. Because of the low Reynolds number laminar flow in the channels, the positive high voltage can be adjusted so that there is very little mixing or cross-contamination of the two fluid streams at the injection point. When the relay connecting the positive high voltage to the CZE buffer reservoir is open, no current and therefore little or no buffer flow from the CZE buffer reservoir to the injection point. Consequently, the sample eluting from the GEMBE channel flows into both the waste and CZE channels (see Fig. 2B). During operation, the relay is left closed for most of the time and is periodically switched to inject a pulse of sample from the GEMBE channel into the CZE channel. Each injected sample pulse then migrates down the CZE channel and mixes with the chiral selector for chiral resolution and, finally, detection.

At the beginning of a separation, a positive pressure is applied to the buffer/waste reservoir to partially counteract the electroosmotic flow, ensuring that the analytes remain in the sample reservoir. Consequently, no analytes reach the injection point,

and no peaks are observed at the detector after the initial CZE injections. Over time the applied pressure is reduced, so that a selected set of analytes can pass through the GEMBE channel to the injection point where they are injected into the CZE channel. The CZE injection is thus selectively biased, with the bias changing with each succeeding injection. For early injections, none or few of the analytes are injected into the CZE channel. Gradually, more of the analytes are injected until all analytes are injected and detected.

The LIF detector signal is recorded throughout the analysis and then split into individual electropherograms for each CZE injection. The raw data corresponding to Fig. 3–7 are included in the ESI†. The electropherograms are then processed to convert the *x*-axis from time to electrokinetic mobility (see above), and they are then assembled into a 2D image such as the one shown in Fig. 3A. The convolution of the GEMBE steps of the first dimension with the CZE peaks of the second dimension gives a result that is visualized as "stripes". Each stripe corresponds to an amino acid or other amine species. The horizontal position of each stripe indicates the amino acid's electrokinetic mobility in the chiral (CZE) separation and the vertical position of the start point of each stripe indicates the amino acid's mobility in the achiral (GEMBE) separation. To help identify peak start points, a derivative can be taken along the vertical dimension of the 2D plot (similar to taking the time derivative of a GEMBE signal) as shown in Fig. 3B.

The resolving power of the 2D separation can be adjusted by varying the acceleration (the rate at which the applied pressure is varied). For rapid acceleration, the 2D separation can be completed in a relatively fast time (18 min for Fig. 3) but gives only a slight improvement in peak capacity over the 1D chiral microchip CZE method (see Discussion). The peak capacity can be improved considerably, however, by using a slower acceleration, though the analysis time is also considerably increased. In practice, a fast separation such as that shown in Fig. 3 is first employed to identify peak positions and regions of interest in the 2D separation space. This is followed by one or more slower separations to provide more detailed information focused on particular regions of interest. Unlike previously described multidimensional separation methods, this optimization can be done simply by changing the starting pressure and acceleration parameter used for the separation rather than by changing hardware or chemical systems.

Fig. 4 shows a high resolution separation of the region of interest around the neutral amino acids: glycine, alanine, serine and valine. All of the neutral amino acid enantiomers that were added to the sample were detectable and resolvable, including both enantiomers of serine and both enantiomers of alanine—something that has not yet been demonstrated in previous work on chiral amino acid separations in microfluidic formats.[32,33,35] In addition, it was also possible to resolve several unknown peaks in this region of interest. These additional species were also found in the analysis of labeled buffer blank samples, indicating either fluorescent or amine impurities in the buffer or impurities in the labeling reagent. The analysis time for this high resolution separation was quite long, requiring almost 3.5 hours. Also apparent in the upper middle portion of Fig. 4B are several "ghost" peaks resulting primarily from the variability of the injection into the 2nd dimension.

Fig. 5 shows a high resolution separation of the region of interest around the acidic amino acids, aspartic acid and glutamic acid, and the peaks resulting from the dye hydrolysis. Again

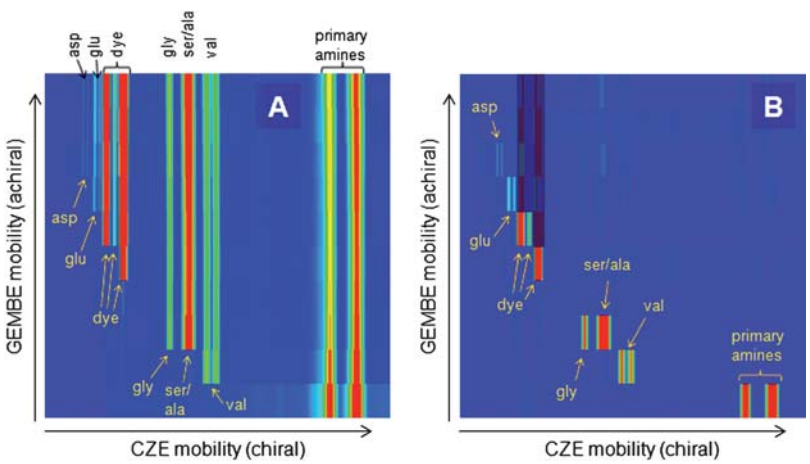

Fig. 3 2D separation result for 200 nmol L^{-1} amino acid analysis. False color images with red corresponding to high brightness. Each known amino acid enantiomer was present in the labeling solution at 10 μmol L^{-1} and diluted 50-fold for analysis. Separation conditions: −4000 V on buffer/waste, +800 V on CZE buffer, sample grounded; pressure applied to buffer/waste was initially +4000 Pa and was reduced at a rate of 5 Pa s^{-1} for 17.7 min; injection into CZE channel was made every 80 s; 0.1 mmol L^{-1} HP-β-CD was added to the CZE buffer. (A) Low resolution 2D "stripe" plot of amino acids and primary amines. Each stripe in the plot corresponds to a fluorescently labeled amine or amino acid. The position of the line along the *x*-axis indicates the amine's mobility in the chiral CZE separation, and the start point of each stripe (indicated with arrows) along the *y*-axis indicates the amine's mobility in the achiral GEMBE separation. Labels indicate the identity of each amine, if known. (B) Low resolution 2D derivative plot. Each amino acid or primary amine corresponds to a spot on the derivative plot, though there are extra spots from fluctuations in the measured intensity of the higher concentration stripes shown in (A). The blanked out regions above the dye peaks are "blind spots" where the detector was saturated because of the high concentration of dye (20 μmol L^{-1}). For the chiral amino acids that were resolved (asp, glu, and val), the L-enantiomer peak is on the left and the D-enantiomer peak is on the right in the figure.

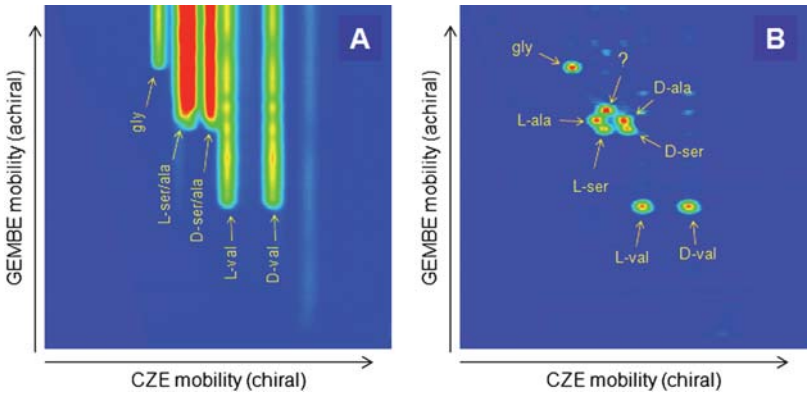

Fig. 4 2D separation result for 190 nmol L^{-1} amino acid analysis. False color images with red corresponding to high brightness. A mixture of labeling solutions was used: each known amino acid enantiomer was present in solution one at 1 μmol L^{-1} and in solution two at 10 μmol L^{-1}. The sample loaded on chip was composed of 9% (v/v) solution one, 1% solution two, and 90% buffer (10-fold dilution of labeling solutions). Separation conditions: −4000 V on buffer/waste, +800 V on CZE buffer, sample grounded; pressure applied to buffer/waste was initially +7900 Pa and was reduced at a rate of 0.25 Pa s^{-1} for 207 min; injection into CZE channel was made every 80 s; 0.3 mmol L^{-1} HP-β-CD was added to the CZE buffer. (A) High resolution 2D "stripe" plot of neutral amino acid region. Each stripe in the plot corresponds to a fluorescently labeled amine or amino acid. The position of the line along the *x*-axis indicates the amine's mobility in the chiral CZE separation, and the start point of each stripe along the *y*-axis indicates the amine's mobility in the achiral GEMBE separation. Arrows indicate the start point of each detected stripe. Labels indicate the identity of each amino acid, if known. (B) High resolution 2D derivative plot. Each amino acid corresponds to a spot on the derivative plot, though there are extra spots from fluctuations in the measured intensity of the higher concentration stripes shown in (A). All of the amino acid enantiomers as well as several unknowns present in the blank were successfully resolved.

all of the amino acid enantiomers were resolved, as well as the dye hydrolysis products (assumed to be the 3 very bright peaks observed in the analysis of labeled buffer blank samples) and 3 unknowns (also found with labeled buffer blank samples, but at lower concentration and/or brightness). The separation time was again quite long, at just under 4 hours.

Note that the cyclodextrin concentration used (0.1 mmol L^{-1} to 0.3 mmol L^{-1}) was an order of magnitude lower than what is typically used for 1D chiral separations.[33,35,42] That is because with the 2D technique, the different amino acids can be resolved in the first dimension, and it is then necessary to use only enough chiral selector to resolve the most difficult enantiomer pair in the second dimension.

In addition to the amino acids that were intentionally added to the sample and the high intensity peaks attributed to dye hydrolysis products, 11 additional species were detectable in the high resolution separations shown in Fig. 4 and 5: eight species in the region of interest around the neutral amino acids and three in

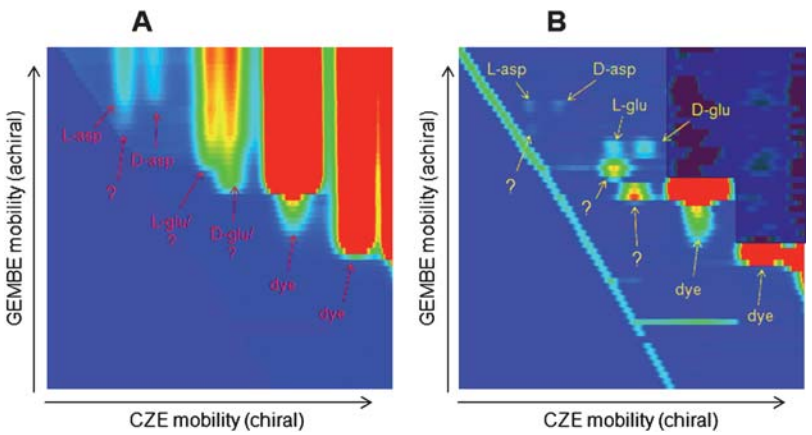

Fig. 5 2D separation result for 100 nmol L^{-1} amino acid analysis. False color images with red corresponding to high brightness. Each known amino acid enantiomer was present in the labeling solution at 1 μmol L^{-1} and diluted 10-fold for analysis. Separation conditions: −4000 V on buffer/waste, +800 V on CZE buffer, sample grounded; pressure applied to buffer/waste was initially +5500 Pa and was reduced at a rate of 0.25 Pa s^{-1} for 238 min; injection into CZE channel was made every 160 s; 0.1 mmol L^{-1} HP-β-CD was added to the CZE buffer. (A) High resolution 2D "stripe" plot of acidic amino acid and free dye region. Each stripe in the plot corresponds to a fluorescently labeled amino acid or dye hydrolysis product (free dye). The position of the line along the *x*-axis indicates the amine's mobility in the chiral CZE separation, and the start point of each stripe along the *y*-axis indicates the amine's mobility in the achiral GEMBE separation. Arrows indicate the start point of each detected stripe. Labels indicate the identity of each amino acid, if known. (B) High resolution 2D derivative plot. Each amino acid corresponds to a spot on the derivative plot. The blanked out regions above the dye peaks are "blind spots" where the detector was saturated because of the high concentration of dye (100 μmol L^{-1}). All of the amino acid enantiomers as well as several unknowns present in the blank were successfully resolved.

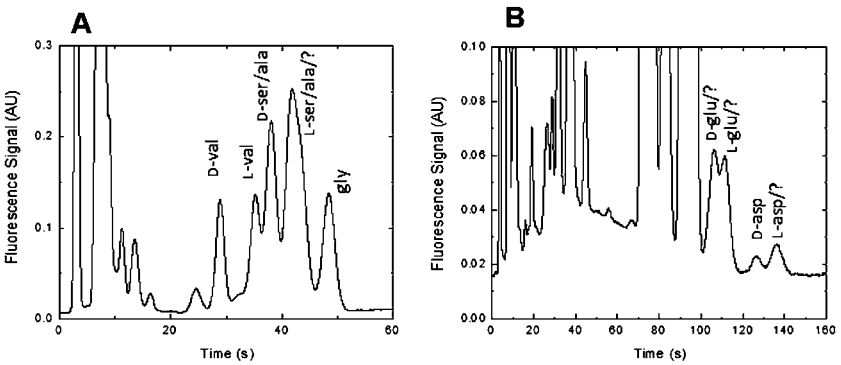

Fig. 6 Two examples of the effect of unidentified impurities on the results of 1D chiral CZE. (A) Neutral amino acids. Same sample as shown in Fig. 4. Note that the coelution of the unknown contaminants with L-alanine and L-serine would potentially lead to a false positive indication of enantiomeric excess. Separation conditions: −4000 V on buffer/waste, +800 V on CZE buffer, sample grounded; pressure applied to buffer/waste was +5100 Pa; 0.3 mmol L^{-1} HP-β-CD was added to the CZE buffer. (B) Acidic amino acids. Same sample as shown in Fig. 5. Note that the coelution of the unknown contaminant with L-aspartic acid would potentially lead to a false positive indication of enantiomeric excess. Separation conditions: −4000 V on buffer/waste, +800 V on CZE buffer, sample grounded; pressure applied to buffer/waste was +2800 Pa; and 0.1 mmol L^{-1} HP-β-CD was added to the CZE buffer.

the region of interest around the acidic amino acids. These unknown species were also detected in labeled buffer blank samples and were present at estimated concentrations ranging from approximately 5 nmol L^{-1} up to 200 nmol L^{-1}.

For amino acid analysis of real samples such as those that might be collected on Mars or elsewhere, care can be taken to eliminate amine contamination from the buffers used for the analysis.[32] However, any real sample (such as from soil, meteorites, or samples that might be collected on the surface of Mars[32–36]) will have interferents that will likely make accurate chiral analyses very difficult without sufficient peak capacity. Therefore, for our 2D analysis, the unknown contaminant species were intentionally left in the system, as a demonstration of how the 2D method could provide improved resolution of enantiomers, even in the presence of several potentially interfering species.

Fig. 6 shows two different examples in which the results of a 1D CZE method appear to show an enantiomeric excess when in fact there is none. Fig. 6A shows the result of a 1D chiral CZE separation of the same sample used for Fig. 4, focused on the region of the electropherogram between val and gly. From the 1D result, it would appear that there is an enantiomeric excess of L-alanine or L-serine (or both). Examination of the 2D plot in Fig. 4 reveals that the apparent enantiomeric excess is actually due to one of the unknown contaminants. Closer examination of the 2D data (see Fig. S5, ESI†) shows that there are actually

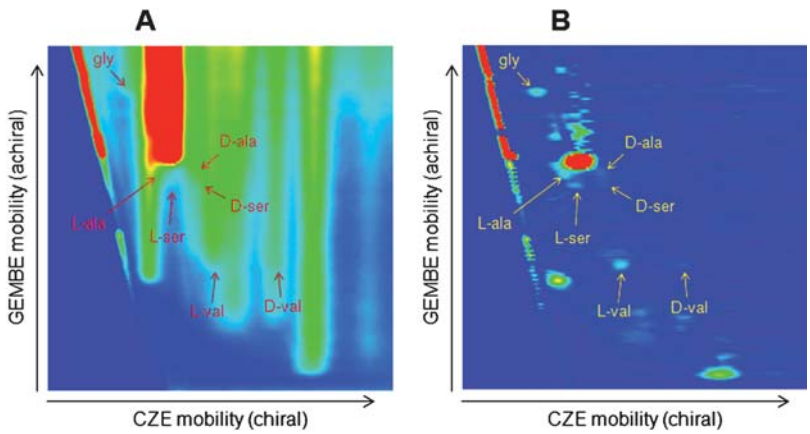

Fig. 7 2D separation result for 10 nmol L^{-1} and 5 nmol L^{-1} amino acid analysis. False color images with red corresponding to high brightness. Each known L-enantiomer and gly was present in the sample at 10 nmol L^{-1}. Each known D-enantiomer was present in the sample at 5 nmol L^{-1}. A mixture of labeling solutions was used: labeling solution one contained each known amino acid enantiomer and gly at 1 μmol L^{-1}, solution two contained each of the D-enantiomers (D-asp, D-glu, D-ser, D-ala, and D-val) at 1 μmol L^{-1}, and solution three was a labeled blank solution (no added amino acids). The sample loaded on chip was composed of 0.5% (v/v) solution one, 0.5% solution two, 9% solution three, and 90% buffer (10-fold dilution of labeling solutions). Separation conditions: −4000 V on buffer/waste, +800 V on CZE buffer, sample grounded; pressure applied to buffer/waste was initially +7900 Pa, and was reduced at a rate of 0.25 Pa s^{-1} for 206 min; injection into CZE channel was made every 60 s; and 0.3 mmol L^{-1} HP-β-CD was added to the CZE buffer. (A) High resolution 2D "stripe" plot of neutral amino acid region with low concentration spiked-in amino acids. Arrows indicate the start point of each detected stripe. Labels indicate the identity of each of the known amino acids. (B) High resolution 2D derivative plot for low concentration spike-in. All of the known amino acid enantiomers were detected. The D-enantiomers were just at the detection limit at a concentration of 5 nmol L^{-1} each. The L-enantiomers and glycine, at 10 nmol L^{-1} each, were clearly detectable.

two unknowns contributing to the apparent excess, one that co-migrates with L-serine and one that co-migrates with L-alanine. A second example is shown in Fig. 6B for a 1D chiral CZE separation focusing on the region around the acidic amino acids. From the 1D separation results, it would appear that there is an excess of the L-enantiomer of aspartic acid. However, as with alanine and serine, the 2D results (Fig. 5) reveal that the apparent excess is actually due to another unknown contaminant. Close examination of the high resolution 2D data (Fig. 4 and 5, and S5, ESI†) shows that for every pair of amino acid enantiomers that we examined, there is at least one interferent that co-migrates in the CZE dimension and could therefore lead to a false positive indication of enantiomeric excess if the 1D method were used.

To examine the potential for the 2D technique to determine enantiomeric ratios in very low concentration samples with possible interferents, a sample was prepared with amino acid enantiomers at a concentration of either 5 nmol L^{-1} or 10 nmol L^{-1}. The concentrations of the L-enantiomers and glycine were 10 nmol L^{-1}, and the concentrations of the D-enantiomers were 5 nmol L^{-1}. The results are shown in Fig. 7. Again, the same set of interferent peaks was present as in every sample examined, including the labeled blank. Even at this very low concentration, each of the amino acids was detected, and it was clear that the L-enantiomers were present at higher concentrations. The L-enantiomers and glycine at 10 nmol L^{-1} were clearly detectable, and the D-enantiomers at 5 nmol L^{-1} were just barely detectable. From these results we conclude that the usable detection limit in this case was about 5 nmol L^{-1}. Note for comparison with previous work that the detection limit ($S/N = 3$) of the instrument used here, estimated for an isolated peak in a single CZE separation, was 300 pmol L^{-1}.

Discussion and conclusions

For separations of amino acids using 1D CZE (or GEMBE, which has similar selectivity), the region of the separation space around the neutral amino acids (between valine and glycine in our examples) is potentially very crowded.[32] Therefore, an important figure of merit is the peak capacity in that region. Published examples of microchip CZE separations of multiple amino acids show peak capacities between valine and glycine ranging from 5 to 10 for achiral separations.[32,36,53] The use of a chiral selector such as a cyclodextrin typically provides better resolution of the neutral amino acids and gives a slightly higher peak capacity. Examples of chiral microchip CZE of amino acids have shown peak capacities between valine and glycine ranging from about 8 to 20.[33,35] By comparison, the peak capacity between D-valine and glycine was about 6 for the CZE dimension in this work.

Of the 50 or so amino acid enantiomers likely to be present in either meteorites or known living systems, approximately half of them will be found in the range between valine and glycine in an achiral CZE separation.[32] Even in the best case of equally distributed peaks, the possible number of species exceeds the peak capacity for what has been demonstrated for 1D microchip CZE. From eqn (1), the fraction of species that will be cleanly resolved from all the others is less than 10%. Other 1D microfluidic techniques have achieved higher peak capacities. For example, the peak capacity between valine and glycine was about 13 for temperature gradient focusing (TGF),[54] and as high as 30 for micellar electrokinetic chromatography (MEKC).[32] However, even with a peak capacity of 30, with 25 randomly located peaks the estimated fraction that will be resolved is less than 20%.

A recently described 2D method using MEKC and CZE on a microchip achieved a peak capacity of approximately 40 between valine and glycine, though without chiral resolution in either dimension.[30] For the 2D method described here, the rectangular area between D-valine and glycine in Fig. 4B has a peak capacity of approximately 70. However, since the GEMBE and CZE dimensions of the separation are not perfectly orthogonal (the detected peaks are clustered along a diagonal line in Fig. 3–5), the rectangular area is an upper bound for the peak capacity. Although a definitive evaluation of the peak capacity would require further work with a more complete selection of amino acids, it can be estimated from the observed spread about the diagonal of the peaks shown in Fig. 4. This gives an estimated peak capacity between valine and glycine of 35. Using eqn (1), the 2D method would be expected to resolve about one quarter of the possible peaks in that range. While this is an improvement over 1D methods, it is not clear whether it is good enough for a conclusive demonstration of an enantiomeric excess in an extraterrestrial sample, for example.

There are a number of potential advantages to the 2D method described here. Because of its simplicity, a multiplexed 2D separation system would be more feasible with this approach. Also, the application of a pressure gradient over time allows for relatively short channels to be used for both the GEMBE and CZE separations, making device design and fabrication less difficult and expensive. In addition to providing resolution in the GEMBE dimension, the applied pressure adjusts the resolution in the CZE dimension so that it is maximized for the set of analytes that require the highest resolution: those that are just eluting from the first dimension GEMBE separation. The method is also fully adjustable requiring only changes to the operational parameters of the method rather than the hardware. The range and resolution of the analysis can be adjusted to suit the needs of a particular sample without making any changes to the hardware.

Two improvements could be made to the hardware used for this work. First, the channel connecting the CZE buffer reservoir to the injection point could be made shorter to eliminate the need for the second (positive) high voltage source. Second, the high voltage power supply(s) and/or the high voltage circuit could be optimized to eliminate the voltage fluctuations that occurred during the switching of the relay. This would reduce or eliminate the peak position and intensity fluctuations that give rise to "ghost" peaks in the 2D plots (see the upper middle portions of Fig. 3B and 4B, for example). A related limitation is the blind areas of the 2D separation space that arise from the high concentration dye hydrolysis peaks (see the upper right corner of Fig. 5B, for example). For trace analysis, when the sample is minimally diluted between labeling and analysis, the dye hydrolysis peaks typically saturate the LIF detection system, and any further increase due to an amine species that coelutes with the dye hydrolysis products would be undetectable. For amino acid analysis, this is not expected to be a serious limitation because the amino acids of interest are typically found in two clusters along the electropherogram: aspartic acid and glutamic

acid in one cluster and most of the others in a cluster between glycine and valine. The dye hydrolysis products are easily resolvable from both of these clusters in the CZE dimension. An additional concern with both this technique and conventional CZE is the stability of the electroosmotic mobility over the time required for many separations. If the electroosmotic mobility drifts over time, the peak positions will shift, making analyte identification problematic.

The biggest drawback to the technique as described here is that it is slow. The results shown in Fig. 4 and 5 each took 3.5 and 4 hours of analysis time. If a more focused region of interest had been used (with GEMBE, the separation can be started and stopped at selected points along the *y*-axis of the 2D plots) that time could possibly have been reduced by a factor of 2. Although this time is significantly less than that required to run a conventional 2D-PAGE separation, it is still considerably longer than is typically considered convenient for microfluidics-based analysis systems.

It seems likely that the speed could be improved, however. For CZE, the time required to achieve a given resolution (or peak capacity) is inversely dependent on the square of the electric field strength used.[55] The estimated field strength in the CZE dimension of the 2D method was 650 V cm^{-1}, which is comparable to the field strength used for much of the recent work by the Mathies group.[32–36,38–40] The time between successive injections was either 80 s or 160 s for the high resolution 2D separations. In contrast, for the optimized 2D MEKC-CZE method described by the Ramsey group,[16] the field strength was 2400 V cm^{-1} and the time between injections was just 1 s. Although a theoretical description of the dependence of analysis time on field strength has not been derived for GEMBE, it appears to follow a power law similar to that for CZE.[46] Consequently, a 10-fold reduction in the time required for both separation dimensions could be achieved with an approximately 3-fold increase in the field strength. Given the moderate field strengths used (160 V cm^{-1} for the GEMBE channel), a 3-fold increase would appear quite feasible. However, to implement the 2D method with a 3-fold increase in the field strength would require a matching 3-fold increase in the applied pressure. This would result in an increase in the Taylor–Aris dispersion[56,57] which would possibly negate any advantage gained by using higher field. In fact, increasing the magnitude of the applied voltage from 4000 V to 5000 V was found experimentally to provide no improvement in resolution for the CZE dimension. Consequently, optimization of this 2D method using the kind of simple device described here would require a more complete theoretical description of the GEMBE technique including such factors as Taylor–Aris dispersion. An alternative approach might be to eliminate the pressure-driven flow component (and therefore the Taylor–Aris dispersion) from the CZE channel by using a track-etched polycarbonate membrane between the GEMBE and CZE channels in an approach similar to the 2D CZE-chiral CZE method that was recently reported.[31]

Acknowledgements

This research was supported by the NASA Astrobiology Science and Technology Instrument Development (ASTID) program grant number NNH06AE121.

References

1 J. C. Giddings, *Unified Separation Science*, John Wiley & Sons, New York, 1991.
2 J. C. Giddings, *Anal. Chem.*, 1984, **56**, 1258A–1270A.
3 P. H. O'Farrell, *J. Biol. Chem.*, 1975, **250**, 4007–4021.
4 T. Stroink, M. C. Ortiz, A. Bult, H. Lingeman, G. J. de Jong and W. J. M. Underberg, *J. Chromatogr., B: Anal. Technol. Biomed. Life Sci.*, 2005, **817**, 49–66.
5 M. Herrero, E. Ibanez, A. Cifuentes and J. Bernal, *J. Chromatogr., A*, 2009, **1216**, 7110–7129.
6 I. Francois, K. Sandra and P. Sandra, *Anal. Chim. Acta*, 2009, **641**, 14–31.
7 K. Sandra, M. Moshir, F. D'Hondt, R. Tuytten, K. Verleysen, K. Kas, I. Francois and P. Sandra, *J. Chromatogr., B: Anal. Technol. Biomed. Life Sci.*, 2009, **877**, 1019–1039.
8 H. J. Cortes, B. Winniford, J. Luong and M. Pursch, *J. Sep. Sci.*, 2009, **32**, 883–904.
9 P. Dugo, F. Cacciola, T. Kumm, G. Dugo and L. Mondello, *J. Chromatogr., A*, 2008, **1184**, 353–368.
10 Y. F. Huang, C. C. Huang, C. C. Hu and H. T. Chang, *Electrophoresis*, 2006, **27**, 3503–3522.
11 S. P. Dixon, I. D. Pitfield and D. Perrett, *Biomed. Chromatogr.*, 2006, **20**, 508–529.
12 J. Szpunar and R. Lobinski, *Anal. Bioanal. Chem.*, 2002, **373**, 404–411.
13 S. Tia and A. E. Herr, *Lab Chip*, 2009, **9**, 2524–2536.
14 H. Chen and Z. H. Fan, *Electrophoresis*, 2009, **30**, 758–765.
15 R. D. Rocklin, R. S. Ramsey and J. M. Ramsey, *Anal. Chem.*, 2000, **72**, 5244–5249.
16 J. D. Ramsey, S. C. Jacobson, C. T. Culbertson and J. M. Ramsey, *Anal. Chem.*, 2003, **75**, 3758–3764.
17 Y. Li, J. S. Buch, F. Rosenberger, D. L. DeVoe and C. S. Lee, *Anal. Chem.*, 2004, **76**, 742–748.
18 S. W. Tsai, M. Loughran and I. Karube, *J. Micromech. Microeng.*, 2004, **14**, 1693–1699.
19 C. Das, J. Zhang, N. D. Denslow and Z. H. Fan, *Lab Chip*, 2007, **7**, 1806–1812.
20 C. A. Emrich, I. L. Medintz, W. K. Chu and R. A. Mathies, *Anal. Chem.*, 2007, **79**, 7360–7366.
21 J. K. Liu, S. Yang, C. S. Lee and D. L. Devoe, *Electrophoresis*, 2008, **29**, 2241–2250.
22 S. Yang, J. K. Liu, C. S. Lee and D. L. Devoe, *Lab Chip*, 2009, **9**, 592–599.
23 J. S. Buch, F. Rosenberger, W. E. Highsmith, C. Kimball, D. L. DeVoe and C. S. Lee, *Lab Chip*, 2005, **5**, 392–400.
24 X. X. Chen, H. K. Wu, C. D. Mao and G. M. Whitesides, *Anal. Chem.*, 2002, **74**, 1772–1778.
25 A. E. Herr, J. I. Molho, K. A. Drouvalakis, J. C. Mikkelsen, P. J. Utz, J. G. Santiago and T. W. Kenny, *Anal. Chem.*, 2003, **75**, 1180–1187.
26 A. Griebel, S. Rund, F. Schonfeld, W. Dorner, R. Konrad and S. Hardt, *Lab Chip*, 2004, **4**, 18–23.
27 Y. C. Wang, M. N. Choi and J. Y. Han, *Anal. Chem.*, 2004, **76**, 4426–4431.
28 K. Usui, A. Hiratsuka, K. Shiseki, Y. Maruo, T. Matsushima, K. Takahashi, Y. Unuma, K. Sakairi, I. Namatame, Y. Ogawa and K. Yokoyama, *Electrophoresis*, 2006, **27**, 3635–3642.
29 Z. Demianova, M. Shimmo, E. Poysa, S. Franssila and M. Baumann, *Electrophoresis*, 2007, **28**, 422–428.
30 B. Xu, X. J. Feng, Y. Z. Xu, W. Du, Q. M. Luo and B. F. Liu, *Anal. Bioanal. Chem*, 2009, **394**, 1911–1917.
31 B. Y. Kim, J. Yang, M. J. Gong, B. R. Flachsbart, M. A. Shannon, P. W. Bohn and J. V. Sweedler, *Anal. Chem.*, 2009, **81**, 2715–2722.
32 T. K. Chiesl, W. K. Chu, A. M. Stockton, X. Amashukeli, F. Grunthaner and R. A. Mathies, *Anal. Chem.*, 2009, **81**, 2537–2544.
33 L. D. Hutt, D. P. Glavin, J. L. Bada and R. A. Mathies, *Anal. Chem.*, 1999, **71**, 4000–4006.
34 A. M. Skelley, H. J. Cleaves, C. N. Jayarajah, J. L. Bada and R. A. Mathies, *Astrobiology*, 2006, **6**, 824–837.
35 A. M. Skelley and R. A. Mathies, *J. Chromatogr., A*, 2003, **1021**, 191–199.
36 A. M. Skelley, J. R. Scherer, A. D. Aubrey, W. H. Grover, R. H. C. Ivester, P. Ehrenfreund, F. J. Grunthaner, J. L. Bada and R. A. Mathies, *Proc. Natl. Acad. Sci. U. S. A.*, 2005, **102**, 1041–1046.

37 A. M. Skelley, F. J. Grunthaner, J. L. Bada, and R. A. Mathies, *First Jet Propulsion Laboratory* in situ *Instruments Workshop*, SPIE-International Society for Optical Engineering, 2003, vol. 4878, pp. 59–67.
38 A. M. Skelley, J. R. Scherer, J. L. Bada, P. Ehrenfreund, F. J. Grunthaner, and R. A. Mathies, *Micro Total Analysis Systems*, Royal Society of Chemistry, 2004, vol. 2, pp. 566–568.
39 A. M. Stockton, T. N. Chiesl, T. K. Lowenstein, X. Amashukeli, F. Grunthaner and R. A. Mathies, *Astrobiology*, 2009, **9**, 823–831.
40 A. M. Stockton, T. N. Chiesl, J. R. Scherer and R. A. Mathies, *Anal. Chem.*, 2009, **81**, 790–796.
41 G. Danger and D. Ross, *Electrophoresis*, 2008, **29**, 4036–4044.
42 G. Danger and D. Ross, *Electrophoresis*, 2008, **29**, 3107–3114.
43 J. L. Bada, *Science*, 1997, **275**, 942–943.
44 J. L. Bada and G. D. McDonald, *Anal. Chem.*, 1996, **68**, A668–A673.
45 D. A. M. Zaia, C. Zaia and H. De Santana, *Origins Life Evol. Biospheres*, 2008, **38**, 469–488.
46 J. G. Shackman, M. S. Munson and D. Ross, *Anal. Chem.*, 2007, **79**, 565–571.
47 D. Ross and J. G. Kralj, *Anal. Chem.*, 2008, **80**, 9467–9474.
48 D. Ross and E. F. Romantseva, *Anal. Chem.*, 2009, **81**, 7326–7335.
49 E. A. Strychalski, A. C. Henry and D. Ross, *Anal. Chem*, 2009, **81**, 10201–10207.
50 S. C. Jacobson, S. V. Ermakov and J. M. Ramsey, *Anal. Chem.*, 1999, **71**, 3273–3276.
51 M. G. Roper, J. G. Shackman, G. M. Dahlgren and R. T. Kennedy, *Anal. Chem.*, 2003, **75**, 4711–4717.
52 G. Ocvirk, T. Tang and D. J. Harrison, *Analyst*, 1998, **123**, 1429–1434.
53 D. J. Harrison, K. Fluri, K. Seiler, Z. H. Fan, C. S. Effenhauser and A. Manz, *Science*, 1993, **261**, 895–897.
54 G. Danger and D. Ross, *Electrophoresis*, 2008, **29**, 3107–3114.
55 J. W. Jorgenson and K. D. Lukacs, *Anal. Chem.*, 1981, **53**, 1298–1302.
56 G. I. Taylor, *Proc. R. Soc. London*, 1953, **219**, 186–203.
57 R. Aris, *Proc. R. Soc. London, Ser. A*, 1956, **235**, 69–77.